

Short Communication

Bivariate colour maps for visualizing climate data

A. J. Teuling,^{a,b,*} R. Stöckli^c and S. I. Seneviratne^a

^a *Institute for Atmospheric and Climate Science, ETH Zurich, Zurich, Switzerland*

^b *Hydrology and Quantitative Water Management Group, Wageningen University, Wageningen, The Netherlands*

^c *MeteoSwiss, Zurich, Switzerland*

ABSTRACT: The increasing availability of gridded, high-resolution, multivariate climatological data sets calls for innovative approaches to visualize inter-variable relations. In this study, we present a methodology, based on properties of common colour schemes, to plot two variables in a single colour map by using a two-dimensional colour legend for both sequential and diverging data. This is especially suited for climate data as the spatial distribution of the relation between different variables is often as important as the distribution of variables individually. Two example applications are given to illustrate the use of the method: one that shows the global distribution of climate based on observed temperature and relative humidity, and the other showing the distribution of recent changes in observed temperature and precipitation over Europe. A flexible and easy-to-implement method is provided to construct different colour legends for sequential and diverging data. Copyright © 2010 Royal Meteorological Society

KEY WORDS mapping; climate zones; climate change

Received 11 August 2009; Revised 27 November 2009; Accepted 19 March 2010

1. Introduction

The increasing availability of gridded, multivariate, climatological data sets calls for new methodologies to visualize and explore the relationships between different variables. These relationships are often difficult to detect when the variables are plotted separately. One particular solution to reduce the dimensionality of the visualization was proposed by Taylor (2001), who showed that all components of the spatial covariance between two variables (i.e. their variances and correlation) can be summarized in a single radial diagram. This type of diagram is especially suited when a suite of different models is evaluated against observations. The spatial structure of the underlying data, however, is not considered. Other solutions for visualization can be found by making use of some of the properties of common colour schemes.

A colour model is a mathematical description of how a colour is constructed from its components. Most colour models have two or more components (or degrees of freedom), for instance, the amount of red, green and blue (RGB model) or the hue, saturation and brightness value (HSV model). Changing any of the components (with some exceptions) results in a different and unique colour. In theory, these degrees of freedom can be utilized to map an equal number of variables to colour, so that all colours on the map correspond to a combination

of variables rather than a single variable. For three degrees of freedom, this requires some way of displaying the legend in more than two dimensions. Triangular colour maps were used previously by Nemani *et al.* (2003, Figure 1A) and Albani *et al.* (2006, Figure 6). The triangular legend, however, has two rather than three degrees of freedom (i.e. the position along two axis of the triangle determines the third), which limits its applicability to variables that always sum up to same number.

In this study, we propose a method that uses a purely two-dimensional (2-D) colour mapping. Its main advantage over other visualization methods is that the distribution of any two variables, along with their covariance, can be condensed in a single map without loss of information and in a way that is easy to interpret (Olsen, 1981). This is illustrated in Figure 1. This method is especially suited to map two variables that are physically linked, but for which their correlation varies regionally. To our best knowledge, such a plot was first used for climate analysis by Teuling *et al.* (2009, Figure 1). In this study, we present more objective and general methods to construct the colour legend than that used by Teuling *et al.* (2009) and provide extended examples for both sequential and diverging data.

2. 1-D and 2-D colour legends

Three main classes of colour legends for thematic maps can be distinguished: sequential, diverging and qualitative

*Correspondence to: A. J. Teuling, Institute for Atmospheric and Climate Science, CHN N 16.2, Universitätstrasse 16, 8092 Zürich, Switzerland. E-mail: ryan.teuling@wur.nl

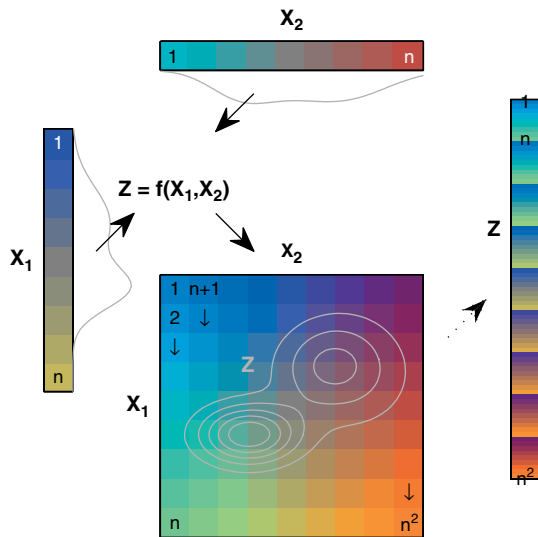


Figure 1. The principle of bivariate colour legends. Two regular variables X_1 and X_2 , which are normally plotted separately using two separate colour legends with resolution n , are combined into a single plotting variable Z to display both variables simultaneously using a single 2-D colour legend. In addition, the colours on the map reflect the covariance structure between X_1 and X_2 (illustrated by grey lines for hypothetical data) and not just their marginal distributions. For compatibility with regular plotting routines, a new 1-D colour legend of size n^2 can be distilled for the plotting variable Z . This figure is available in colour online at www.interscience.wiley.com/ijoc

(Brewer *et al.*, 2003). In this study, we focus on the first two classes. Sequential data differs from diverging data in that it is insensitive to any offset (e.g. temperature). In contrast, diverging data diverges from a reference level (often zero), e.g. anomalies, trends, errors or correlations. Sequential data are best plotted using a limited number of hues and/or a constant gradient in luminance, whereas diverging data are best plotted with contrasting hues and decreasing luminance on both sides of the origin. Here, luminance refers to ‘whiteness’ that results from a particular combination of RGB components.

We considered several aspects in the construction of the 2-D colour legends. Firstly, the method should create uniform gradients in both hue and luminance to avoid the suggestion of non-physical gradients in the data. Secondly, the legend should contain multiple contrasting hues to make optimum use of the available colour space. Thirdly, the method should be independent of the resolution of the legend for maximum flexibility. In general, colour legends with high dimensionality are more suited for qualitative representation, whereas maps with a limited dimension of the colour table are more easily interpreted quantitatively (Brewer *et al.*, 2003). In Section 3, we will provide examples of both. Finally, a similar procedure for the diverging and sequential legends would ease both implementation and interpretation.

Our method represents the individual components of the RGB model by linear surfaces in the considered domain of the bivariate space (see Appendix A). A ‘whitening kernel’ (illustrated in Figure 4(c)) as a function of distance to the origin is applied to the sequential

colour legend. It changes the origin colour to white, while keeping the original colours in the corners. The method preserves uniqueness in colours and allows (for sequential data) for an increase in luminance gradient to capture information about form (spatial distribution) and value as effectively as possible (Ware, 1988). A drawback is that at maximum, only one primary colour (i.e. red, green or blue) can be produced due to additional mixing of non-zero components (a result from the constraint of linear surfaces). Also, although our maps can be used safely on most media, more sophisticated methods would be needed to preserve contrasts and uniqueness of colour across all platforms and media (Robertson and O’Callaghan, 1986).

For compatibility with common plotting routines, a 1-D colour legend can be constructed that links a single plotting variable $Z = 1, 2, 3, \dots, n \times n$ (where n is the number of rows or columns in the 2-D colour legend) to the two physical variables X_1 and X_2 . This is illustrated in Figure 1. Note that the spatial field of the plotting variable Z itself is non-continuous, and that continuity is apparent only in the colour distribution. As a result, no contouring algorithms can be used on Z , but only on X_1 and/or X_2 .

3. Example applications

3.1. Global climate distribution

An example of a sequential bivariate colour map is given in Figure 2, where the concurrent global distribution of temperature (T) and relative humidity (RH) is shown. The data are gridded observations (10’ spatial resolution) for the period 1961–1990 compiled by the Climate Research Unit (New *et al.*, 2002, Mitchell and Jones, 2005). Temperature and relative humidity are appropriate variables for bivariate mapping, as they have a clear physical link and their correlation changes regionally (i.e. on a global scale both hot and dry, and hot and humid regions occur). Note that whereas traditionally temperature and precipitation are used for the primary delineating climate zones (as in the Köppen–Geiger classification; Peel *et al.*, 2007), the distribution of relative humidity will generally follow that of precipitation.

Figure 2 illustrates well the strong variations in the relationship between temperature and humidity. Firstly, (dark) magenta regions indicate hot and humid regions. These occur in Amazonia, Central Africa and Southeast Asia. Orange regions are characterized by high average temperatures but low humidity. This combination is typical for subtropical deserts and occurs in the central Sahara, the Northern Arabian Peninsula, Australia, the Kalahari and the Sonoran Desert in North America. Blue colours indicate humid and cooler climate zones, whereas darker colours (e.g. Central Europe) indicate higher temperatures than that indicated by light blue (e.g. Greenland). Finally, the combination of cool temperatures and moderate to low humidity is rare, and occurs only in and around the main mountain ranges (e.g. Tibetan

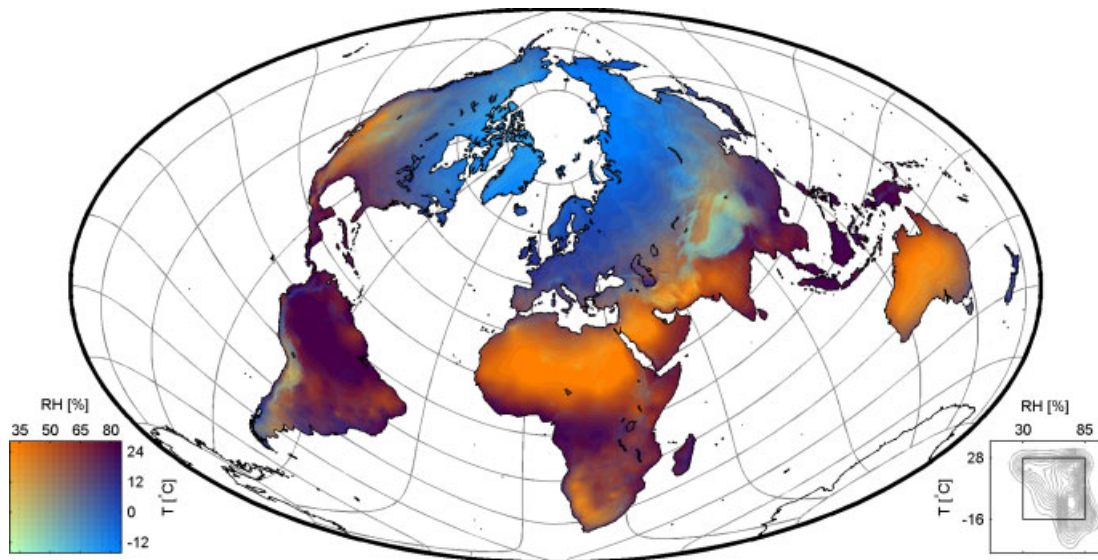


Figure 2. Distribution of the world's climate zones based on observed average near-surface temperature (T) and relative humidity (RH) for the period 1961–1990. The map was plotted using the equal-area Briesemeister projection to minimize distortion both around the North Pole and the Equator (note that no data is available for Antarctica). The inset shows the bivariate frequency distribution and limits of the colour legend. The distribution is based on the original data set and is not corrected for area. Parameters used for plotting are $n = 16$ and $a = 0.72$. Source: Climate Research Unit (CRU) high-resolution climate data (version 2.1). This figure is available in colour online at www.interscience.wiley.com/ijoc

Plateau and Andes). Note that because humidity and temperature are the two main determinants of climate, the resulting continuous bivariate map matches the distribution of discrete climate zones derived from more complex classifications (Peel *et al.*, 2007).

The distribution of climate zones is non-uniform (see bivariate frequency distribution, inset Figure 2) and has distinct peaks at extreme combinations of T and RH. The bivariate distribution is also a practical tool to determine the appropriate plotting limits. Choosing too wide limits reduces the colour contrast in the map, whereas too narrow limits remove the contrast in the extreme regions. In this study, the limits were chosen such that most colours occur in the map, while at the same time the size of the regions without contrast (i.e. Sahara and Amazonia) is limited.

3.2. Recent climate change in Europe

An illustration of the use of a bivariate diverging colour scheme is given in Figure 3. Here, we show the observed trends in near-surface climate for Europe over the past 30 years (1979–2008) based on data from the European Climate Assessment & Dataset (Haylock *et al.*, 2008). When trends in temperature (T) and precipitation (P) are considered on an annual timescale, the distribution across Europe is fairly homogeneous (not shown). However, when the trends are considered for each season separately, considerable regional variability in the distribution and even in the sign of the trends becomes apparent. Temperature and precipitation trends can be linked through different processes, i.e. they might both be caused by changes in circulation or SST, or decreasing precipitation might induce higher temperatures due to reduced evaporation in water-limited environments

(Seneviratne *et al.*, 2006). This behaviour makes temperature and precipitation trends suitable for plotting on a bivariate colour map.

In Figure 3, white indicates areas where no change in either precipitation or temperature has been observed. Magenta indicates regions where both precipitation and temperature show an increasing trend, and orange indicates regions where an increase in temperature is accompanied by a decrease in precipitation. Yellow and red regions are dominated by a decrease in precipitation and an increase in temperature, respectively. In winter (December–February), there is a strong north–south gradient in the climate trends (Figure 3(a)). Large positive winter temperature trends in Scandinavia are accompanied by large positive trends in precipitation, while at the same time the Mediterranean shows little warming but a large decrease in precipitation. The Baltic area shows a strong winter warming but a decrease in precipitation.

In spring (March–May; Figure 3(b)), an east–west gradient in the trends exists. West Europe experienced a warming, with increasing drying towards the Mediterranean, whereas most change in Eastern Europe is in precipitation rather than in temperature. In summer (June–August; Figure 3(c)), most of Europe has warmed considerably. A similar strong drying trend as that observed for spring is found along the Mediterranean, whereas in Central Europe summer precipitation has slightly increased. The warming and drying are less pronounced during autumn (September–November; Figure 3(d)), when temperature trends around the Mediterranean are small and precipitation shows an increase in parts of the Iberian Peninsula and the Balkan region. Only Scandinavia shows a warming trend in autumn.

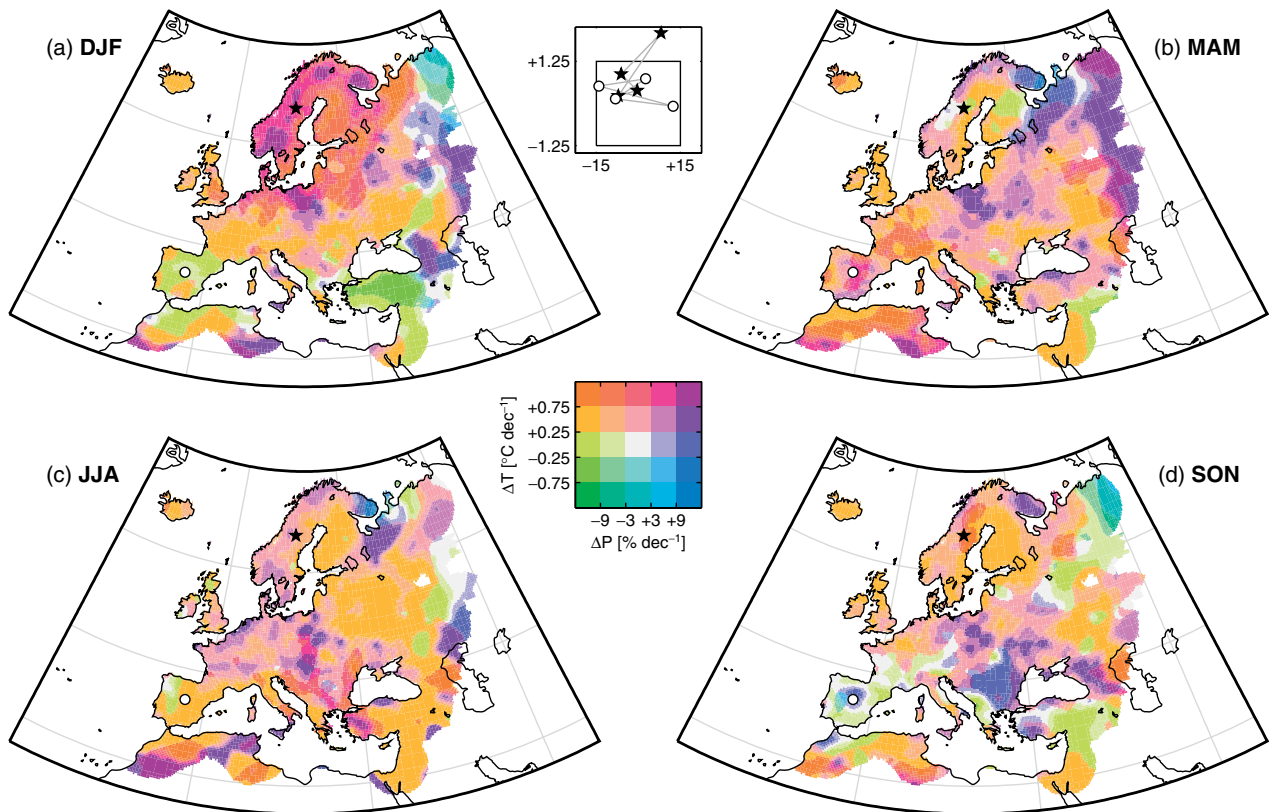


Figure 3. Recent trends in Europe's climate as diagnosed by observed temperature (T) and precipitation (P) over the 30-year period 1979–2008. Trends are determined for each season separately using linear regression of season mean values. Inset shows the seasonal trends for two points in Scandinavia (★) and on the Iberian Peninsula (○). Colours along the southern and eastern boundaries might be affected by interpolation. Parameters used for plotting are $n = 5$ and $a = 0.37$. Source: E-OBS data set from the ENSEMBLES project provided by the European Climate Assessment & Dataset (version 2.0). This figure is available in colour online at www.interscience.wiley.com/ijoc

4. Discussion

The method presented in this study allows for plotting of two variables on one map without loss of information. Its main advantage is that it condenses data of several plots into one by using colour, thus allowing for direct and intuitive evaluation of relationships between variables in relation to their geographical distribution. The method works both for sequential and diverging map data.

Inevitably, bivariate maps are more difficult to interpret than the univariate counterparts. Therefore, more attention should be paid to their production. Although our method is easy to implement and produces fair results on most media, it has two major drawbacks. Firstly, by making use of the RGB model, the colour legends are not device independent. Secondly, our method does not yet consider colour perception. This can lead to subjective interpretation of maps with diverging legends in particular. Therefore, we encourage further development towards bivariate colour legend definitions that are both device independent and produce large yet perceptually constant gradients in hue and luminance.

All figures in this study were produced using the same script that includes some additional options. This script (programmed in MATLAB) is available from the authors upon request.

Appendix A

A1. Construction of 2-D color legend

We construct sequential colour legends by linear interpolation of the individual components of the RGB colour model (Figure 4). The surfaces are chosen such that in three of the corners, each of the colour components has its maximum intensity (1), whereas in the opposite corner the intensity is zero (Figure 4(a) and (b)). As a result, the colour in the centre of the colour legend is always medium grey (50% intensity). Also, luminance changes along one parallel, but not along the other. For diverging colour legends, we adjust the colours resulting from the linear interpolation by adding a 'whitening kernel' to each component (Figure 4(c)). This changes the grey at the origin to white (for $a = 0.5$), whereas in the corners the colours remain unchanged. This method produces constant colour gradients in two dimensions, but the possible colour combinations are limited to three because 'opposite' to any colour component can only be the two other components or a mixture of them (Figures 1 and 2 give two of the three possibilities).

Some flexibility is added by introducing a parameter (a) that controls the slope of the two off-diagonal surfaces (red and blue in Figure 4). The parameter a controls the luminance gradient along the main diagonal of the colour scheme. When $a = 1$, the lower and upper diagonal

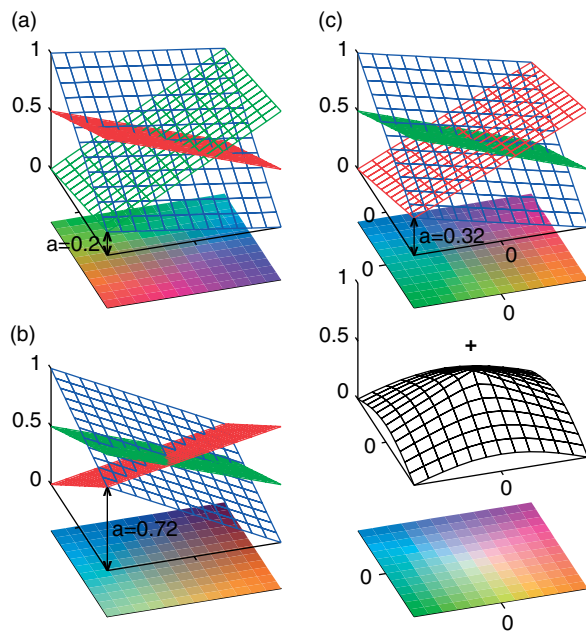


Figure 4. Construction of bivariate colour legends. (a and b) Examples for sequential colour legends. (b) is used in Figure 2. (c) Two-step construction of the diverging legend used in Figure 3. The parameter a controls the luminance gradient along the diagonal. Note that $a = 0.25$ results in equal luminance in all corners, but that at the same time $a \neq 0.5$ limits the effectiveness of the whitening kernel. This figure is available in colour online at www.interscience.wiley.com/ijoc

corners become white and black, respectively. When $a = 0.5$, the diagonal corners have the most contrast in hue. When $a = 0.25$, all corners have the same luminance. When $a = 0$, one of the primary colours results in the lower-left corner (red in case of Figure 4(a)).

Acknowledgements

We acknowledge the E-OBS data set from the EU-FP6 project ENSEMBLES (<http://www.ensembles-eu.org>) and the data providers in the ECA&D project (<http://eca.knmi.nl>). A. J. T. acknowledges partial financial support from

the Netherlands Organisation for Scientific Research (NWO) through a Rubicon grant.

References

- Albani M, Medvigy D, Hurtt GC, Moorcroft PR. 2006. The contributions of land-use change, CO₂ fertilization, and climate variability to the Eastern US carbon sink. *Global Change Biology* **12**(12): 2370–2390.
- Brewer CA, Hatchard GW, Harrower MA. 2003. ColorBrewer in print: a catalog of color schemes for maps. *Cartography and Geographic Information Science* **30**(1): 5–32.
- Haylock MR, Hofstra N, Klein Tank AMG, Klok EJ, Jones PD, New M. 2008. A European daily high resolution gridded data set of surface temperature and precipitation for 1950–2006. *Journal of Geophysical Research* **113**: D20119, DOI:10.1029/2008JD010201.
- Mitchell TD, Jones PD. 2005. An improved method of constructing a database of monthly climate observations and associated high-resolution grids. *International Journal of Climatology* **25**: 693–712, DOI:10.1002/joc.1181.
- Nemani RR, Keeling CD, Hashimoto H, Jolly WM, Piper SC, Tucker CJ, Myneni RB, Running SW. 2003. Climate-driven increases in global terrestrial net primary production from 1982 to 1999. *Science* **300**: 1560–1563, DOI:10.1126/science.1082750.
- New M, Lister D, Hulme M, Makin I. 2002. A high resolution data set of surface climate over global land areas. *Climate Research* **21**: 1–25.
- Olsen JM. 1981. Spectrally encoded two-variable maps. *Annals of the Association of American Geographers* **71**(2): 259–276.
- Peel MC, Finlayson BL, McMahon TA. 2007. Updated world map of the Köppen-Geiger climate classification. *Hydrology and Earth System Sciences* **11**: 1633–1644.
- Robertson PK, O'Callaghan JF. 1986. The generation of color sequences for univariate and bivariate mapping. *IEEE Computer Graphics* **6**(2): 24–32.
- Seneviratne SI, Lüthi D, Litschi M, Schär C. 2006. Land-atmosphere coupling and climate change in Europe. *Nature* **443**(7108): 205–209, DOI:10.1038/nature05095.
- Taylor KE. 2001. Summarizing multiple aspects of model performance in a single diagram. *Journal of Geophysical Research* **106**(D7): 7183–7192, DOI: 10.1029/2000JD900719.
- Teuling AJ, Hirschi M, Ohmura A, Wild M, Reichstein M, Ciais P, Buchmann N, Ammann C, Montagnani L, Richardson AD, Wohlfahrt G, Seneviratne SI. 2009. A regional perspective on trends in continental evaporation. *Geophysical Research Letters* **36**: L02404, DOI:10.1029/2008GL036584.
- Ware C. 1988. Color sequences for univariate maps: Theory, experiments and principles. *IEEE Computer Graphics* **8**(5): 41–49.